Article

Selective Fluorimetric Detection of Pyrimidine Nucleotides in Neutral Aqueous Solution with a Styrylpyridine-Based Cyclophane

Julika Schlosser, Julian F. M. Hebborn, Daria V. Berdnikova [ID] **and Heiko Ihmels *** [ID]

Department of Chemistry-Biology, Research Center of Micro- and Nanochemistry and (Bio)Technology (Cμ), University of Siegen, Adolf-Reichwein-Str. 2, 57068 Siegen, Germany; julika.schlosser@uni-siegen.de (J.S.)
* Correspondence: ihmels@chemie.uni-siegen.de; Tel.: +49-271-740-3440

Abstract: A styrylpyridine-containing cyclophane with diethylenetriamine linkers is presented as a host system whose association with representative nucleotides was examined with photometric and fluorimetric titrations. The spectrometric titrations revealed the formation of 1:1 complexes with log K_b values in the range of 2.3–3.2 for pyrimidine nucleotides TMP (thymidine monophosphate), TTP (thymidine triphosphate) and CMP (cytidine monophosphate) and 3.8–5.0 for purine nucleotides AMP (adenosine monophosphate), ATP (adenosine triphosphate), and dGMP (deoxyguanosine monophosphate). Notably, in a neutral buffer solution, the fluorimetric response to the complex formation depends on the type of nucleotide. Hence, quenching of the already weak fluorescence was observed with the purine bases, whereas the association of the cyclophane with pyrimidine bases TMP, TTP, and CMP resulted in a significant fluorescence light-up effect. Thus, it was demonstrated that the styrylpyridine unit is a useful and complementary fluorophore for the development of selective nucleotide-targeting fluorescent probes based on alkylamine-linked cyclophanes.

Keywords: fluorescent dyes; nucleotide recognition; heterocycles; host–guest chemistry

1. Introduction

Nucleotides play a crucial role in several biological processes, for example as essential building blocks in DNA replication and RNA synthesis [1,2]. Furthermore, they are essential in cell signaling, metabolism, and enzyme reactions as cofactors for NAD^{+} and FAD and as energy carriers in the form of triphosphate nucleotides [3,4]. Therefore, the detection and monitoring of nucleotides are important tasks to contribute to the assessment and understanding of biochemical processes in living organisms [5–9]. Along these lines, photometric and electrochemical analysis, as well as ^{1}H NMR spectroscopic analysis, are routinely used methods for nucleotide detection; however, elaborate protocols, relatively expensive equipment, and limited sensitivity are drawbacks of these methods [10,11]. For this purpose, fluorescence spectroscopy is a useful and easily accessible analytical tool because it enables the efficient and sensitive detection of biologically relevant analytes with suitable fluorescent probes (chemosensors), which change their emission properties upon analyte binding [12–20]. Along these lines, fluorescent probes that can detect nucleotides by means of emission quenching or emission enhancement (light up) have been reported [21–24]. However, selective chemosensors for particular nucleotides are still needed, so the development of such fluorescent probes still represents a rewarding and challenging research field in chemistry [25–27].

The most abundant nucleotide is adenosine triphosphate (ATP), which plays an important role in the energy transport in living organisms [28,29] and as a main biochemical component in cancer cells, where it can either enhance or suppress tumor growth, depending on the concentration [30]. Consequently, several different methods and approaches for the efficient and selective detection of ATP have been reported [31–38]. On the contrary, the selective analysis and sensing of other nucleotides has been scarcely reported so far.

For example, the selective photometric detection of thymidine triphosphate (TTP) relative to other mono-, di-and triphosphate nucleotides has been realized with gold nanoparticles and a *p*-xylylbis(Hg^{2+}-cyclen) complex [39]. Likewise, cytidine triphosphate (CTP) has been shown to induce selective luminescence quenching of a terbium(III)-organic framework [40], and a polyhydroxy-substituted Schiff base receptor has been reported to be a selective fluorescent chemosensor for CTP and ATP [41]. More recently, a bisnaphthalimide receptor with a pyridine spacer has been introduced as a selective fluorescent probe for CTP [42]. Moreover, anthracene derivatives with two appended imidazolium groups have been reported whose emission is efficiently quenched by GTP [43].
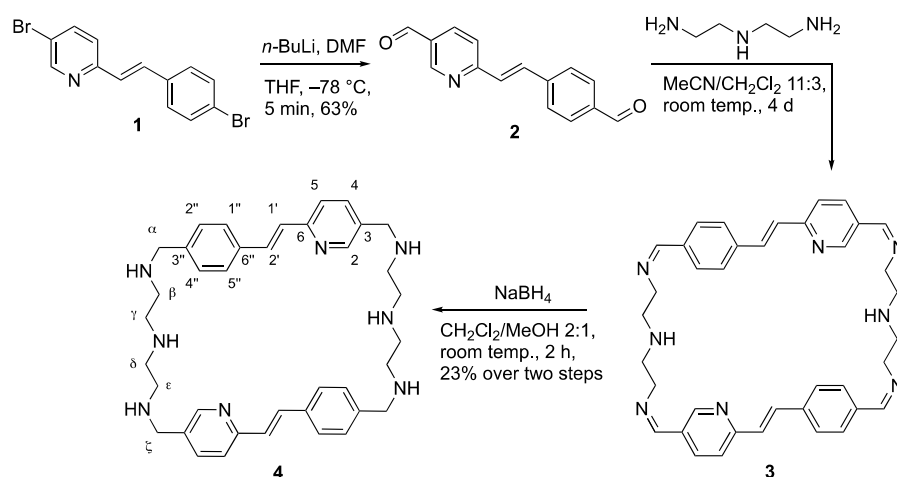
In this context, fluorescent cyclophanes have been established as useful scaffolds for the development of host systems for inorganic and organic anions and may be applied in chemosensing, bioimaging, and drug delivery [44–52]. In particular, several phenyl- [53,54], naphthalene- [55], anthracene- [56–58], and acridine-based [59] cyclophanes, as well as metallocyclophanes [60], have been reported as hosts that strongly bind to nucleotides [25,61]. In seminal work, bisnaphthalenophanes with six amino-functionalities in the linking chains have been introduced as ideal host molecules for the efficient recognition of organic and inorganic phosphates [55]. Likewise, it has been shown that similar anthracene- [62] and pyrene-based [63–65] cyclophanes have the ability to discriminate between different nucleotide triphosphates by the selective complex formation and that these interactions may be used for fluorimetric detection of nucleotides [44,61]. Besides the recognition of single nucleotides, cyclophanes are also apt to bind preferentially to nucleobases in mismatched and abasic site-containing DNA [66–69].

Although some cyclophanes are already available for fluorimetric nucleotide detection, there is still room for further development. Specifically, variations of the aromatic unit appear promising because this part of the host molecule provides an essential binding site for π stacking with the nucleic base. Surprisingly, most employed aromatic subunits are fused polycyclic fragments with limited conformational flexibility, such as naphthalene or anthracene, whereas more flexible scaffolds with resembling π surface, such as stilbenes or styryl-substituted hetarenes, have not been employed for this purpose, so far. Along these lines, we proposed that the known 2-styrylpyridine unit may serve as a useful, complementary aromatic component in nucleotide-binding cyclophanes because it provides a flexible aromatic surface, which may enable a more variable π stacking, along with a decent dipole, which may increase the binding affinity by dipole-dipole interactions with the nucleic base. Herein, we report on the synthesis of a bis-styrylpyridine-based cyclophane, and demonstrate that it may be used for fluorimetric detection and differentiation of nucleotides at physiological pH.

2. Results

2.1. Synthesis

The known dibromostyrylpyridine derivative **1** [70] was formylated by lithium-halogen exchange with *n*-BuLi and subsequent reaction with DMF to the corresponding styrylpyridine bis-carbaldehyde **2** in 63% yield (Scheme 1, see Supplementary Materials). Condensation of the latter with diethylenetriamine and subsequent reduction of the tetraimine intermediate **3** with NaBH$_4$ gave the macrocyclic polyamine **4** in a yield of 23%. The known derivative **1** was synthesized by a varied procedure and identified by comparison with the literature data [71], and the new compounds **2** and **4** were identified and fully characterized by NMR spectroscopy (^{1}H, ^{13}C, COSY, HSQC, and HMBC), elemental analyses, and mass spectrometry (Figures S2–S7). In all cases, the *E*-configuration of the alkene units in compounds **1**, **2**, and **4** were indicated by characteristic coupling constants of the alkene protons ($^3J_{H–H}$ = 16 Hz).

Scheme 1. Synthesis of cyclophane **4**.

2.2. Solvent and pH-Dependent Absorption and Emission Properties

In the MeOH solution, cyclophane **4** exhibited an absorption maximum at λ_{abs} = 314 nm and a fluorescence maximum at λ_{fl} = 379 nm with low emission quantum yield (<0.01) (see Supplementary Materials).

The pH dependence of the absorption properties of cyclophane **4** was determined by spectrometric acid-base titrations in Britton-Robinson buffer (Figure 1). At neutral pH, the absorption maximum was at λ_{abs} = 314 nm. The absorbance increased both at lower (pH < 5) and higher pH (>8) values, with the highest absorbance at pH 2. The absorption maximum also shifted with varying pH, from λ_{abs} = 321 nm at pH 2 to λ_{abs} = 314 nm at pH 7 and to λ_{abs} = 318 nm at pH 12. Furthermore, a slight shoulder at λ_{abs} = 364 nm was observed at pH 2, which steadily disappeared with increasing pH.
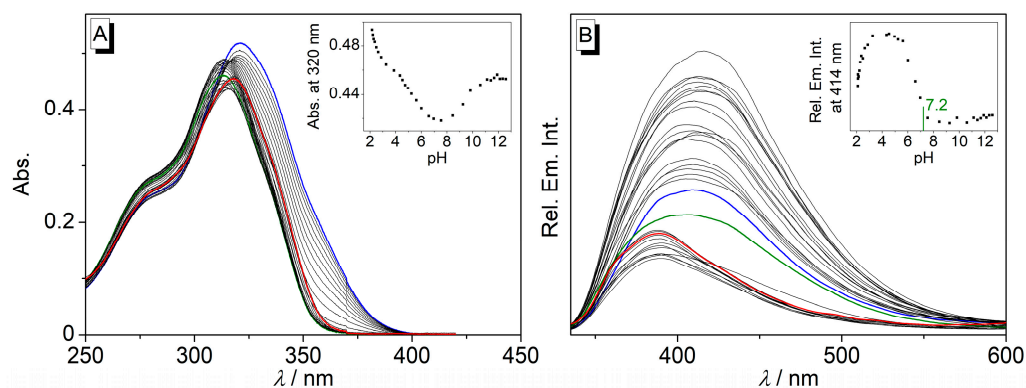

Figure 1. Photometric (**A**) and fluorimetric (**B**) acid–base titrations of cyclophane **4**. Blue line: beginning of titration (pH = 2.0); green line: absorbance and emission at pH 7.2; red line: end of titration (pH = 12.6). Insets: plot of the absorbance at 320 nm (**A**) and fluorescence at 414 nm (**B**) versus pH. In all cases: c = 10 μM, in Britton-Robinson buffer with 5% DMSO, λ_{ex} = 313 nm.

The data from the photometric titration were used to determine the pK_a values of 5.2 and 9.4. Another pK_a value was estimated to be in the range of 2–3, as has been usually observed for resembling cyclophanes with the same diethylenetriamine linker [62]; however, no adequate fit was obtained for this region, so a more accurate value was not available.

The emission spectrum of cyclophane **4** revealed a broad maximum at λ_{fl} = 410 nm at pH 2. With increasing pH to 4, the emission intensity firstly increased by a factor of ca. 2 and reached the highest intensity with a bathochromic shift of $\Delta\lambda_{fl}$ = 5 nm. With the further addition of base (pH > 4), the fluorescence was strongly quenched by about 70% with a

hypsochromic shift of the emission maximum of $\Delta\lambda = 27$ nm at pH 8.5. At pH > 9, the emission intensity remained low, with a slight increase in the emission after pH > 10. Most notably, at neutral pH, the emission of the styrylpyridine is already sufficiently quenched so this compound may be used as a fluorescence light-up probe for target nucleotides at a physiological pH range, that is, under conditions usually found in real biological samples.

2.3. Nucleotide-Binding Properties of 4

The association of the macrocyclic polyamine **4** with selected nucleotides was investigated by photometric and fluorimetric titrations with adenosine monophosphate (AMP), ATP, deoxyguanosine monophosphate (dGMP), thymidine monophosphate (TMP), TTP, and CTP in cacodylate buffer solution at pH 7.2, that is, conditions at which the emission is already very low (Figures 2 and 3). Upon addition of AMP, ATP, and dGMP to **4**, the absorbance ($\lambda_{max} = 314$ nm) decreased with the formation of a red-shifted absorption band ($\Delta\lambda = 5$ nm) and isosbestic points at $\lambda = 323$ nm, 320 nm, and 320 nm, respectively (Figure 2A). In the presence of these nucleotides, the already weak fluorescence of the cyclophane **4** was further quenched with different efficiencies, that is, with I/I_0 of 0.46 (AMP), 0.59 (ATP), and 0.04 (dGMP) at saturation (Figures 2B and 4A). Moreover, the fluorescence maximum of styrylpyridine **4** was blue-shifted with $\Delta\lambda = 34$ nm on the addition of AMP and ATP, whereas no shift of the fluorescence maximum was observed with dGMP.
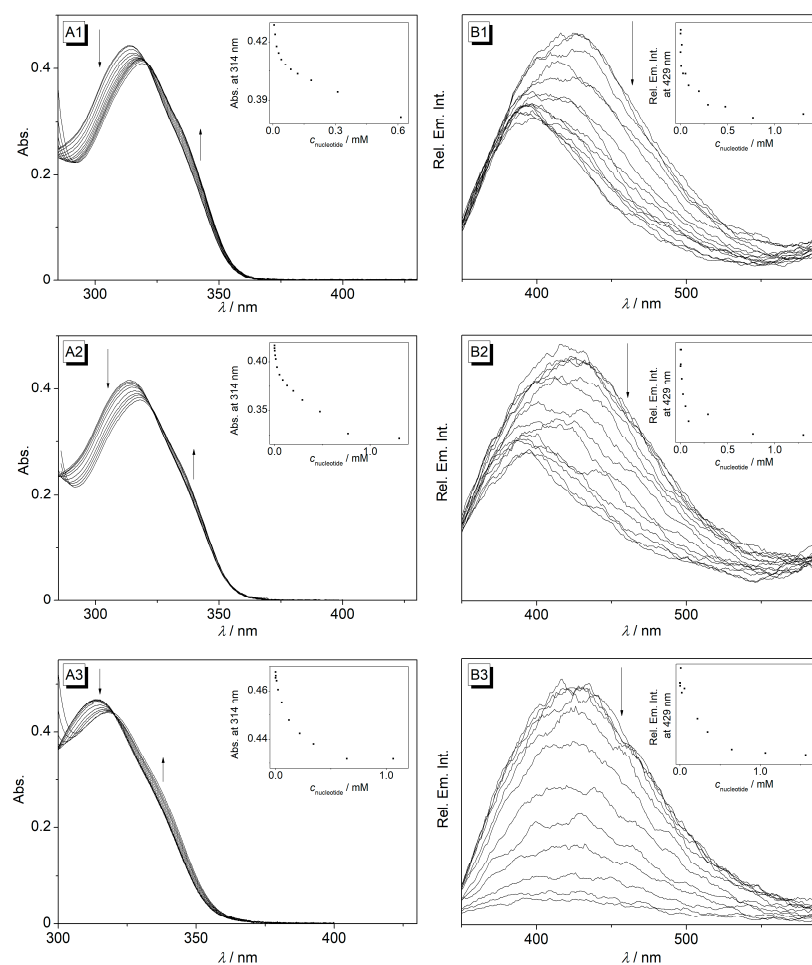

Figure 2. Photometric (**A**) and fluorimetric (**B**) titrations of cyclophane **4** ($c = 10$ μM) with ATP (**1**), AMP (**2**), and dGMP (**3**) in cacodylate buffer (pH 7.2); $T = 20\ °C$; $\lambda_{ex} = 314$ nm. The arrows indicate the changes in absorption and emission upon the addition of nucleotides. Inset: plot of the absorption at 314 nm versus nucleotide concentration.

Figure 3. Photometric (**A**) and fluorimetric (**B**) titrations of cyclophane **4** (c = 10 μM) with TMP (**1**), TTP (**2**), and CMP (**3**) in cacodylate buffer (pH 7.2); T = 20 °C; λ_{ex} = 314 nm. The arrows indicate the changes in absorption and emission upon the addition of nucleotides. Inset: plot of the absorption at 314 nm versus nucleotide concentration.
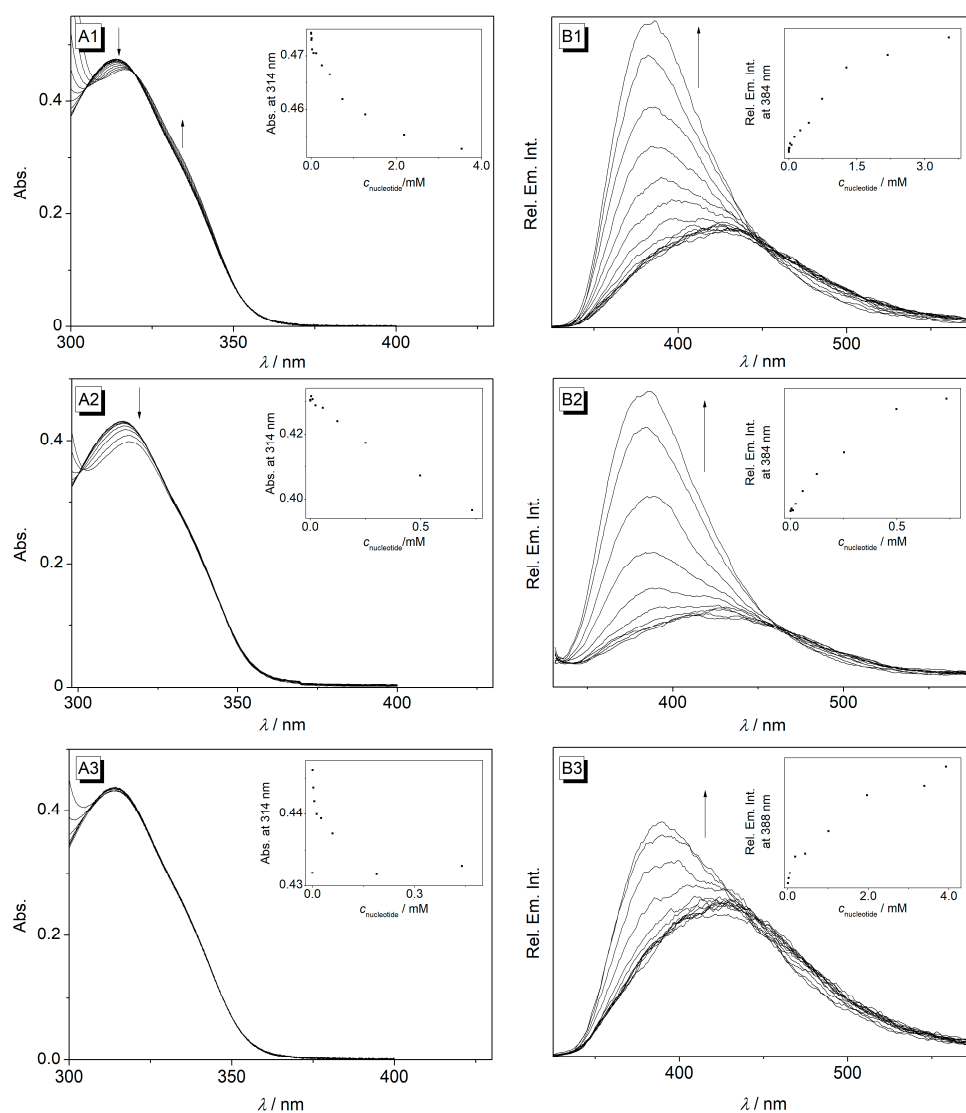

Figure 4. (**A**) Changes of relative emission intensity, I/I_0, of cyclophane **4** (c = 10 μM) upon addition of nucleotides, blue: TTP (detector limit reached at $c_{nucleotide}$ = 0.24 mM), black: TMP, red: CMP, green: ATP (saturation reached at $c_{nucleotide}$ = 0.22 mM), magenta: AMP, orange: dGMP; in cacodylate buffer (pH 7.2); T = 20 °C; λ_{ex} = 314 nm. (**B**) Pictures of the emission color of **4** in cacodylate buffer (left) and in the presence of CMP (middle) and TMP (right).

The binding constants were determined from the experimental binding isotherms of the photometric titrations. Thus, the experimental data were reasonably fitted to a 1:1 binding stoichiometry of nucleotide and **4** with $\log K_b$ values of 4.1, 5.0, and 3.8 for AMP, ATP, and dGMP, respectively (Table 1). These values are in the same range of $\log K_b$ values for two resembling pyrene-based diethylenetriamine-cyclophanes with $\log K_b$ values of 3.00 and 4.15 with AMP, 5.48 and 5.55 with ATP and 3.51 and 4.50 with dGMP [63] and slightly higher than those observed with the resembling anthracene-based cyclophane with a $\log K_b$ value of 3.38 with ATP [62]. In comparison with mono- and triphosphate nucleotides, higher binding constants were also obtained with ATP as compared with AMP [63].

Table 1. Absorption and emission properties of cyclophane **4** and its complexes with nucleotides, and the corresponding binding constants, $\log K_b$.

	λ_{abs}/nm [a]	$\Delta\lambda_{abs}$/nm	λ_{fl}/nm [a]	$\Delta\lambda_{fl}$/nm	$\log K_b$ [b]	I/I_0
4	314 (4.67) [c]	–	429 (<0.01) [d]	–	–	–
4/TMP	317	3	384	−45	2.8 ± 0.1	2.72
4/TTP	317	3	384	−45	3.2 ± 0.1	2.43
4/CMP	314	–	388	−41	2.3 ± 0.1	1.23
4/AMP	319	5	395	−34	4.1 ± 0.1	0.48
4/ATP	319	5	395	−34	5.0 ± 0.1	0.54
4/dGMP	319	5	429	–	3.8 ± 0.1	0.10

[a] In cacodylate buffer, pH 7.2; T = 20 °C. [b] Determined from the analysis of the fluorimetric titration data with Specfit/32™ with adequate fits for complexes with **4**:nucleotide ratio 1:1. K in M^{-1}. [c] Molar extinction coefficient ε, given as lg ε, ε in cm^{-1} M^{-1}. [d] Fluorescence quantum yield, relative to naphthalene (ϕ_{fl} = 0.23 in cyclohexane, ref. [72]), λ_{ex} = 280 nm, estimated error: ± 10% of the given value.
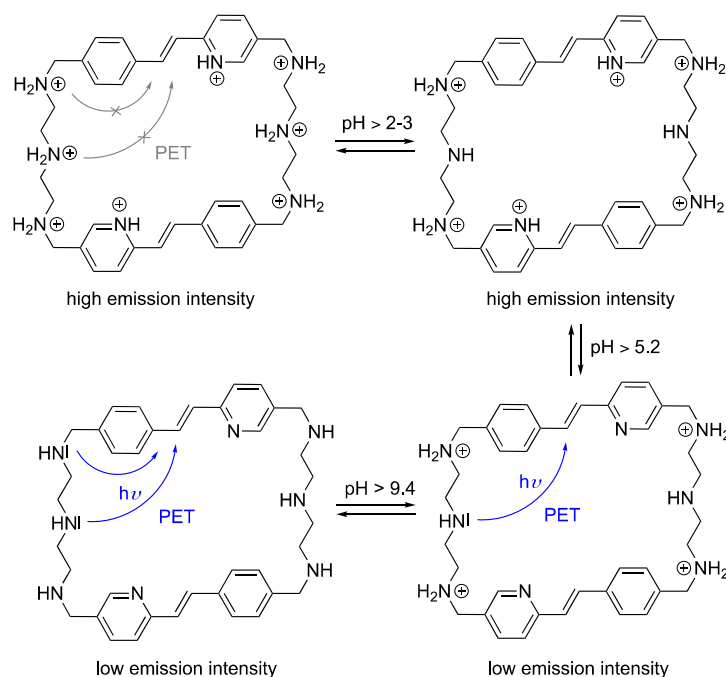
Titrations of the cyclophane **4** with TMP and TTP decreased the absorbance with red shifts of $\Delta\lambda$ = 3 nm (Figure 3A). However, in contrast to titrations with the other nucleotides (see above), the addition of TMP and TTP resulted in a significant increase and blue shift ($\Delta\lambda$ = 45 nm) of the fluorescence band (Figure 3B). The fluorescence light-up effect is more pronounced with TMP (I/I_0 = 2.72) than with TTP (I/I_0 = 2.43), respectively (Figure 4A). Upon the addition of CMP to **4**, the absorption band remained essentially unchanged. At the same time, a fluorescence light-up effect was observed upon the addition of CMP along with a blue shift of the fluorescence maximum of $\Delta\lambda$ = 41 nm; however, the increase of the fluorescence intensity (I/I_0 = 1.23) was less pronounced than the one with TMP and TTP (Figure 4). Notably, the increased emission intensity of compound **4** upon complex formation with the pyrimidine nucleotides can be seen with the naked eye (Figure 4B). From the fluorimetric titration data, the limit of detection (LOD) of **4** was estimated to be 0.09 μM, 0.02 μM, and 0.04 μM for TMP, TTP, and CMP, respectively (Table S1).

The binding isotherms were determined from the fluorimetric titration data as $\log K_b$ = 2.8, 3.2, and 2.3 for 1:1 complexes with TMP, TTP, and CMP, respectively (Table 1, Figure S1). For comparison, the reported $\log K_b$ values of resembling pyrene- and anthracene-based cyclophanes are 4.77 and 5.16 [63], and 3.60 [62] for complexes with TTP, that is, somewhat higher than the values for cyclophane **4**. Furthermore, the binding constants for cyclophane **4** are higher for the complexes with purine nucleotides than for the pyrimidine nucleotides, which is in accordance with a literature-known pyrene-based cyclophane [63].

3. Discussion

The pK_a values of 2–3, 5.2, and 9.4 for cyclophane **4** are assigned to the eight available protonation sites, namely the amine and pyridine functionalities. Specifically, the pK_a values of the secondary amines fall in the range of the ones of similar, known amino-containing macrocyclic structures [63]. Accordingly, the pK_a values of the two central amino groups are estimated to be in the range of 2–3, and the pK_a value of 9.4 is assigned to the four lateral amino groups. In addition, the pK_a value of 5.2 relates to the two pyridine units, which is in accordance with the known pK_a value of 5.0 for 2-styrylpyridine [73].
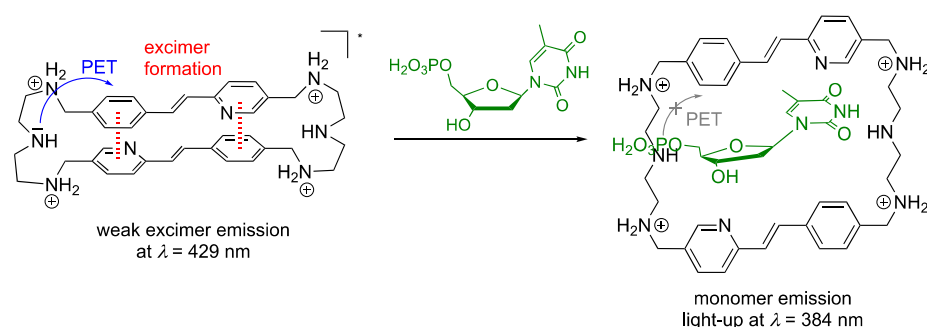
Overall, the acid-base titrations revealed the expected protolytic equilibrium resulting from the protonation of the amino functionalities and the pyridine unit in an acidic medium (Scheme 2). In particular, as has been shown for resembling fluorophore-containing polyamine-linked cyclophanes [62,74], the emission of the styrylpyridine is efficiently quenched by a photoinduced electron transfer (PET) reaction of the electron-donating amine functionalities with the excited fluorophore, whereas upon protonation this deactivation pathway is suppressed and the emission intensity increases significantly [75]. Apparently, the pyridine unit does not interfere with this general process; however, under acidic conditions, the formation of the corresponding pyridinium may be responsible for the shifts of the emission maximum at lower pH values [76].

Scheme 2. Protolytic equilibrium of cyclophane **4**.

As compared with resembling anthracene- and pyrene-based cyclophanes, which show a fluorescence light-up effect upon complexation of TTP, CTP, and ATP and fluorescence quenching with GTP [62,63], cyclophane **4** exhibits a different dependence of the fluorimetric response on the type of nucleotide. Namely, a fluorescence enhancement occurs upon binding of pyrimidine nucleotides TMP, TTP, and CMP, whereas an effective quenching of the fluorescence results from association with purine nucleotides AMP, ATP, and dGMP. This observation may be explained by the specific pH- and structure-dependent emission properties of the cyclophane **4**. Firstly, the amino functionalities of the linker units quench the emission of such cyclophanes by a PET reaction (see above) [62], which readily explains the low emission at the applied pH of 7.2. More importantly, cyclophane **4** exhibits two different emission maxima: a fluorescence maximum at $\lambda = 429$ nm in the unbound state and a blue-shifted one around $\lambda = 384$ nm upon complexation of the nucleotides. As it has been observed already with similar aminoalkyl-linked cyclophanes that these compounds tend to form emitting excimers [63], it is proposed that the red-shifted emission of **4** also originates from an intramolecular excimer formation between the two styrylpyridine units (Scheme 3). This proposal is in agreement with the excimer formation of resembling azastilbene-type derivatives, which is accompanied by a red shift of the emission maximum [77–80]. Upon binding of the pyrimidine nucleobases with the cyclophane **4**, the emission increases as a result of the formation of the host-guest complexes, presumably because the complexation of the nucleotide involves hydrogen bonding with the amino functionalities [81,82], which in turn suppresses the PET quenching of the photoexcited

fluorophore and leads to increased fluorescence intensity. In addition, the accommodation of the nucleotide in the cavity of the cyclophane also inhibits the excimer formation so only the blue-shifted monomer emission is detected. In contrast, the binding of purine nucleobases leads to emission quenching of cyclophane **4**. This fluorescence quenching of cyclophane **4** by purine nucleotides may be explained by a different binding mode of the purine nucleotides ATP, AMP, and dGMP, as compared with one of pyrimidine nucleotides, which leads to a fluorescence enhancement upon formation of the cyclophane-nucleotide complex [83–85]. At the same time, it cannot be excluded that the purine nucleotides bind in a similar mode as the pyrimidine nucleotides and that the fluorescence quenching by ATP, AMP, and dGMP is just the result of a stronger quenching efficiency of the purine bases. Accordingly, the latter have a much lower reduction potential than the pyrimidine bases [86,87] and can, therefore, induce an efficient fluorescence quenching by a photoinduced electron transfer reaction with the excited styrylpyridine.

Scheme 3. Formation of excimer complex of cyclophane **4** and proposed binding mode of pyrimidine nucleotide TMP (green) with **4** (* indicates the excited state).

To the best of our knowledge, this is the first reported cyclophane-based fluorescent probe that can discriminate between purine and pyrimidine nucleobases based on a clear light-up effect induced by the latter. Nevertheless, a resembling anthracene-based derivative bearing two imidazolium-containing alkyl chains is known to show these properties [43]. Because of the significant light-up effect of **4** upon binding to TMP and TTP, cyclophane **4** may be employed as a fluorescent probe for the detection of thymine-based nucleotides. Notably, the detection of nucleotides is accomplished under physiological conditions at pH 7.2, rendering cyclophane **4** also interesting for biological applications. For comparison, only a few examples of cyclophanes have been explicitly reported that enable the detection of nucleotides at neutral pH [54,88], so there is still a demand to develop such recognition systems for nucleotides, that is, as the one reported herein, which operate in a physiological pH range.

4. Conclusions

The spectroscopic investigation of the nucleotide-binding properties of the cyclophane **4** revealed that purine bases AMP, ATP, and dGMP are binding upon fluorescence quenching, whereas in contrast, with pyrimidine bases TMP, TTP, and CMP, a clear, distinguishable fluorescence light-up effect was observed. Overall, we have demonstrated that the styrylpyridine unit is a useful and complementary fluorophore for the development of selective nucleotide-targeting fluorescent probes based on alkylamino-linked cyclophanes, especially considering the observation that this probe operates at the physiological pH range. Therefore, further studies of the particular binding modes as well as systematic variations of the substitution pattern, should enable the development of efficient chemical sensors for bioanalytical applications.

5. Materials and Methods

The commercially available chemicals (Alfa, Merck, Fluorochem, or BLDpharm) were of reagent grade and used without further purification. Nucleotides ATP (adenosine-5′-

triphosphate disodium salt) and CMP (cytidine-5′-monophosphate disodium salt) were purchased from Feinbiochemika (Heidelberg, Germany), and nucleotides TMP (thymidine-5′-monophosphate disodium salt hydrate), TTP (thymidine-5′-triphosphate tetrasodium salt), AMP (adenosine-5′-monophosphate sodium salt) and dGMP (2′-deoxyguanosine-5′-monophosphate sodium salt hydrate) were purchased from Sigma-Aldrich (St. Louis, MO, USA). ^{1}H NMR spectra were recorded with a JEOL ECZ 500 (^{1}H: 500 MHz and ^{13}C: 125 MHz) and a Varian VNMR S600 (^{1}H: 600 MHz and ^{13}C: 150 MHz) at T = 25 °C. The ^{1}H NMR and ^{13}C{1H} NMR spectra were referenced to an internal standard in CDCl$_3$ [TMS: $\delta(^1$H) = 0.00 ppm, $\delta(^{13}$C) = 0.00 ppm]. Structures were assigned with additional information from gCOSY, gHSQC, and gHMBC experiments, and the spectra were processed with the software MestreNova. The mass spectra were recorded with a Finnigan LCQ Deca (driving current: 6 kV, collision gas: argon, capillary temperature: 200 °C, support gas: nitrogen) and an Orbitrap mass spectrometer Thermo Fisher Exactive (driving current: 3.5 kV, capillary temperature: 300 °C, capillary voltage: 45 V, injection rate: 5 μL/min, scanning range: 150−750 m/z, and resolution: ultra-high) and processed with the software Xcalibur. The CHNS analysis data were determined in-house with a HEKAtech EuroEA combustion analyzer. The melting points were measured with a melting point apparatus BÜCHI 545 (Büchi, Flawil, CH) and are uncorrected. The absorption spectra were recorded on a Varian Cary 100 Bio absorption spectrometer with Hellma quartz glass cuvettes 110-QS (layer thickness d = 10 mm). The emission spectra were recorded on a Varian Cary Eclipse fluorescence spectrometer with Hellma quartz glass cuvettes 115 FQS (layer thickness d = 10 mm). All measurements were recorded at T = 20 °C as adjusted with a thermostat if not stated otherwise. The sample solutions in the titration experiments were mixed with a reaction vessel shaker Top-Mix 11118 (Fisher Bioblock Scientific). E-Pure water was obtained with an ultrapure water system D 4632-33 (Wilhelm Werner GmbH, Leverkusen, D) with filters D 0835, D 0803, and D 5027 (2×).

Synthesis of (12E,25E)-1^1,3,6,9,14^1,16,19,22-Octaazapentacyclo-1,14(3,6)-dipyridina-11,24(1,4)-dibenzenacyclo-hexacosaphane-12,25-diene (**4**)

Under an argon gas atmosphere, a solution of 2 (100 mg, 420 μmol) in CH$_2$Cl$_2$ (15 mL) and MeCN (55 mL) was added dropwise to a solution of ethylentriamine (45.4 μL, 43.5 mg, 420 μmol) in MeCN (30 mL) at room temperature, and the mixture was stirred for 4 d at room temperature. Approximately half the volume of the solvent was removed under reduced pressure, and the precipitated solid was filtered off, washed with MeCN (2 × 10 mL), dried under reduced pressure (0.5 mbar, 1 h), and suspended in a mixture of CH$_2$Cl$_2$ (5 mL) and MeOH (2.5 mL). NaBH$_4$ (100 mg, 2.66 mmol) was added, and the mixture was stirred at room temperature for 3 h under an argon gas atmosphere. The solvent was removed under reduced pressure, and the remaining residue was dissolved in aqueous NaOH (20 mL, 1.0 M) and extracted with CHCl$_3$ (3 × 20 mL). The combined organic layers were dried with K$_2$CO$_3$ and filtered, and the solvent was removed under reduced pressure. The crude product was dissolved in CHCl$_3$ (5 mL), precipitated with hexane (25 mL), filtered off and recrystallized from toluene to give the product 4 as light yellow amorphous solid (60 mg, 97 μmol, 23%); mp 184–187 °C.-^{1}H NMR (500 MHz, CDCl$_3$): δ = 1.74 (br s, 6H, 6 × NH), 2.76–2.82 (m, 8H, 4 × CH$_2$, γ-H, δ-H, fornumbering, see Scheme 1), 2.83–2.92 (m, 8H, 4 × CH$_2$, β-H, ε-H), 3.77 (s, 8H, 4 × CH$_2$, α-H, ζ-H), 7.11, 7.12 (2 × d, ^3J = 16 Hz, 2H, 1′-H), 7.16, 7.23 (2 × d, ^3J = 8 Hz, 2H, 5-H), 7.26, 7.28 (2 × d, ^3J = 8 Hz, 4H, 2″-H, 4″-H), 7.43, 7.45 (2 × d, ^3J = 8 Hz, 4H, 1″-H, 5″-H), 7.52–7.57 (m, 2H, 4-H), 7.57, 7.60 (2 × d, ^3J = 16 Hz, 2H, 2′-H), 8.52 (s, 2H, 2-H).-^{13}C NMR (125 MHz, CDCl$_3$): δ = 48.3, 2 × 48.4 (4 × C, Cγ, Cδ), 48.8, 2 × 48.9 (4 × C, Cβ, Cε), 51.0 (2 × C, Cζ), 53.6 (2 × C, Cα), 121.8, 121.9 (2 × C, C5), 127.1, 127.2 (4 × C, C1″, C5″), 127.4, 127.5 (2 × C, C1′), 2 × 128.4 (4 × C, C2″, C4″), 132.0, 132.1 (2 × C, C2′), 2 × 134.2 (2 × C, C3), 2 × 135.4 (2 × C, C6″), 136.2, 136.3 (2 × C, C4), 140.7, 140.8 (2 × C, C3″), 2 × 149.4 (2 × C, C2), 154.5, 154.6 (2 × C, C6).-MS (ESI$^+$): m/z (%) = 617 (100) [M + H]$^+$.-El. Anal. for C$_{38}$H$_{48}$N$_8$ × H$_2$O calc. (%): C 71.89, H 7.94, N 17.65, found: C 72.11, H 7.68, N 17.07.

Supplementary Materials: The following supporting information can be downloaded at: https://www.mdpi.com/article/10.3390/chemistry5020082/s1, Synthesis of **1** and **2** [71]; determination of fluorescence quantum yields [72]; Figure S1: Plot of fluorescence intensity at selected wavelength versus concentration of nucleotides; Figure S2: ^{1}H-NMR spectrum of **1**; Figure S3: ^{13}C-NMR spectrum of **1**; Figure S4: ^{1}H-NMR spectrum of **2**; Figure S5: ^{13}C-NMR spectrum of **2**; Figure S6: ^{1}H-NMR spectrum of **4**; Figure S7: ^{13}C-NMR spectrum of **4**; Table S1: Limit of detection [89,90].

Author Contributions: Conceptualization, J.S. and H.I.; methodology, J.S. and H.I.; experimental work (synthesis, analysis, documentation), J.S.; experimental work (synthesis) J.F.M.H.; experimental work (calculation of binding constants), D.V.B.; writing—original draft preparation, J.S.; writing—review and editing, H.I.; project administration, H.I.; funding acquisition, H.I. All authors have read and agreed to the published version of the manuscript.

Data Availability Statement: Data are available from the authors.

Conflicts of Interest: The authors declare no conflict of interest.

Sample Availability: Samples are not available from the authors.

References

1. Lane, A.N.; Fan, T.W.-M. Regulation of mammalian nucleotide metabolism and biosynthesis. *Nucleic Acids Res.* **2015**, *43*, 2466–2485. [CrossRef] [PubMed]
2. Berdis, A. Nucleobase-modified nucleosides and nucleotides: Applications in biochemistry, synthetic biology, and drug discovery. *Front. Chem.* **2022**, *10*, 1051525. [CrossRef] [PubMed]
3. Hirsch, A.K.H.; Fischer, F.R.; Diederich, F. Phosphate recognition in structural biology. *Angew. Chem. Int. Ed.* **2007**, *46*, 338–352. [CrossRef]
4. Illes, P.; Klotz, K.-N.; Lohse, M.J. Signaling by extracellular nucleotides and nucleosides. *Naunyn Schmiedebergs Arch. Pharmacol.* **2000**, *362*, 295–298. [CrossRef]
5. Florea, M.; Nau, W.M. Implementation of anion-receptor macrocycles in supramolecular tandem assays for enzymes involving nucleotides as substrates, products, and cofactors. *Org. Biomol. Chem.* **2010**, *8*, 1033–1039. [CrossRef]
6. Ojida, A.; Takashima, I.; Kohira, T.; Nonaka, H.; Hamachi, I. Turn-On Fluorescence Sensing of Nucleoside Polyphosphates Using a Xanthene-Based Zn(II) Complex Chemosensor. *J. Am. Chem. Soc.* **2008**, *130*, 12095–12101. [CrossRef] [PubMed]
7. Malojčić, G.; Piantanida, I.; Marinić, M.; Žinić, M.; Marjanović, M.; Kralj, M.; Pavelić, K.; Schneider, H.-J. A novel bis-phenanthridine triamine with pH controlled binding to nucleotides and nucleic acids. *Org. Biomol. Chem.* **2005**, *3*, 4373–4381. [CrossRef]
8. Sakamoto, T.; Ojida, A.; Hamachi, I. Molecular recognition, fluorescence sensing, and biological assay of phosphate anion derivatives using artificial Zn(ii)–Dpa complexes. *Chem. Commun.* **2009**, *2*, 141–152. [CrossRef]
9. Hewitt, S.H.; Ali, R.; Mailhot, R.; Antonen, C.R.; Dodson, C.A.; Butler, S.J. A simple, robust, universal assay for real-time enzyme monitoring by signalling changes in nucleoside phosphate anion concentration using a europium(iii)-based anion receptor. *Chem. Sci.* **2019**, *10*, 5373–5381. [CrossRef]
10. Sessler, J.L.; Gale, P.; Cho, W.-S. *Anion Receptor Chemistry*; The Royal Society of Chemistry: London, UK, 2006.
11. Wu, Q.; Lei, Q.; Zhong, H.-C.; Ren, T.-B.; Sun, Y.; Zhang, X.-B.; Yuan, L. Fluorophore-based host-guest assembly complexes for imaging and therapy. *Chem. Commun.* **2023**, *59*, 3024–3039. [CrossRef]
12. Niu, H.; Liu, J.; O'Connor, H.M.; Gunnlaugsson, T.; James, T.D.; Zhang, H. Photoinduced electron transfer (PeT) based fluorescent probes for cellular imaging and disease therapy. *Chem. Soc. Rev.* **2023**, *52*, 232–2357. [CrossRef] [PubMed]
13. Klymchenko, A.S. Fluorescent Probes for Lipid Membranes: From the Cell Surface to Organelles. *Acc. Chem. Res.* **2023**, *56*, 1–12. [CrossRef] [PubMed]
14. Luo, C.; Zhang, Q.; Sun, S.; Li, H.; Xu, Y. Research progress of auxiliary groups in improving the performance of fluorescent probes. *Chem. Commun.* **2023**, *59*, 2199–2207. [CrossRef] [PubMed]
15. Fang, H.; Chen, Y.; Jiang, Z.; He, W.; Guo, Z. Fluorescent Probes for Biological Species and Microenvironments: From Rational Design to Bioimaging Applications. *Acc. Chem. Res.* **2023**, *56*, 258–269. [CrossRef] [PubMed]
16. Neto, B.A.D.; Correa, J.R.; Spencer, J. Fluorescent Benzothiadiazole Derivatives as Fluorescence Imaging Dyes: A Decade of New Generation Probes. *Chem. Eur. J.* **2022**, *28*, e202103262. [CrossRef]
17. Manna, S.K.; Mondal, S.; Jana, B.; Samanta, K. Recent advances in tin ion detection using fluorometric and colorimetric chemosensors. *New J. Chem.* **2022**, *46*, 7309–7328. [CrossRef]

18. Krämer, J.; Kang, R.; Grimm, L.M.; de Cola, L.; Picchetti, P.; Biedermann, F. Molecular Probes, Chemosensors, and Nanosensors for Optical Detection of Biorelevant Molecules and Ions in Aqueous Media and Biofluids. *Chem. Rev.* **2022**, *122*, 3459–3636. [CrossRef]

19. Niko, Y.; Klymchenko, A.S. Emerging solvatochromic push-pull dyes for monitoring the lipid order of biomembranes in live cells. *J. Biochem.* **2021**, *170*, 163–174. [CrossRef]

20. Klymchenko, A.S. Solvatochromic and Fluorogenic Dyes as Environment-Sensitive Probes: Design and Biological Applications. *Acc. Chem. Res.* **2017**, *50*, 366–375. [CrossRef]

21. Hargrove, A.E.; Nieto, S.; Zhang, T.; Sessler, J.L.; Anslyn, E.V. Artificial Receptors for the Recognition of Phosphorylated Molecules. *Chem. Rev.* **2011**, *111*, 6603–6782. [CrossRef]

22. Kataev, E.A.; Shumilova, T.A.; Fiedler, B.; Anacker, T.; Friedrich, J. Understanding Stacking Interactions between an Aromatic Ring and Nucleobases in Aqueous Solution: Experimental and Theoretical Study. *J. Org. Chem.* **2016**, *81*, 6505–6514. [CrossRef] [PubMed]

23. Suzuki, Y.; Masuko, M.; Hashimoto, T.; Hayashita, T. Selective ATP recognition by boronic acid-appended cyclodextrin and a fluorescent probe supramolecular complex in water. *New J. Chem.* **2023**, *47*, 7035–7040. [CrossRef]

24. Kuchelmeister, H.Y.; Schmuck, C. Molecular Recognition of Nucleotides. In *Designing Receptors for the Next Generation of Biosensors*; Piletsky, S.A., Whitcombe, M.J., Eds.; Springer: Berlin/Heidelberg, Germany, 2013; pp. 53–65. ISBN 978-3-642-32329-4.

25. Agafontsev, A.M.; Ravi, A.; Shumilova, T.A.; Oshchepkov, A.S.; Kataev, E.A. Molecular Receptors for Recognition and Sensing of Nucleotides. *Chem. Eur. J.* **2019**, *25*, 2684–2694. [CrossRef] [PubMed]

26. Li, W.; Gong, X.; Fan, X.; Yin, S.; Su, D.; Zhang, X.; Yuan, L. Recent advances in molecular fluorescent probes for organic phosphate biomolecules recognition. *Chin. Chem. Lett.* **2019**, *30*, 1775–1790. [CrossRef]

27. Yue, Y.; Huo, F.; Cheng, F.; Zhu, X.; Mafireyi, T.; Strongin, R.M.; Yin, C. Functional synthetic probes for selective targeting and multi-analyte detection and imaging. *Chem. Soc. Rev.* **2019**, *48*, 4155–4177. [CrossRef] [PubMed]

28. Fontecilla-Camps, J.C. The Complex Roles of Adenosine Triphosphate in Bioenergetics. *ChemBioChem* **2022**, *23*, e202200064. [CrossRef] [PubMed]

29. Pontes, M.H.; Sevostyanova, A.; Groisman, E.A. When Too Much ATP Is Bad for Protein Synthesis. *J. Mol. Biol.* **2015**, *427*, 2586–2594. [CrossRef]

30. Vultaggio-Poma, V.; Sarti, A.C.; Di Virgilio, F. Extracellular ATP: A Feasible Target for Cancer Therapy. *Cells* **2020**, *9*, 2496. [CrossRef]

31. Khojastehnezhad, A.; Taghavi, F.; Yaghoobi, E.; Ramezani, M.; Alibolandi, M.; Abnous, K.; Taghdisi, S.M. Recent achievements and advances in optical and electrochemical aptasensing detection of ATP based on quantum dots. *Talanta* **2021**, *235*, 122753. [CrossRef]

32. Wu, Y.; Wen, J.; Li, H.; Sun, S.; Xu, Y. Fluorescent probes for recognition of ATP. *Chin. Chem. Lett.* **2017**, *28*, 1916–1924. [CrossRef]

33. Kumar, P.; Pachisia, S.; Gupta, R. Turn-on detection of assorted phosphates by luminescent chemosensors. *Inorg. Chem. Front.* **2021**, *8*, 3587–3607. [CrossRef]

34. Jun, Y.W.; Sarkar, S.; Kim, K.H.; Ahn, K.H. Molecular Probes for Fluorescence Imaging of ATP in Cells and Tissues. *ChemPhotoChem* **2019**, *3*, 214–219. [CrossRef]

35. Huang, B.; Liang, B.; Zhang, R.; Xing, D. Molecule fluorescent probes for adenosine triphosphate imaging in cancer cells and in vivo. *Coord. Chem. Rev.* **2022**, *452*, 214302. [CrossRef]

36. Butler, S.J.; Jolliffe, K.A. Anion Receptors for the Discrimination of ATP and ADP in Biological Media. *ChemPlusChem* **2021**, *86*, 59–70. [CrossRef] [PubMed]

37. Zhou, X.; Shang, L. Recent Advances in Nanomaterial-based Luminescent ATP Sensors. *Curr. Anal. Chem.* **2022**, *18*, 677–688. [CrossRef]

38. Bazzicalupi, C.; Bencini, A.; Giorgi, C.; Valtancoli, B.; Lippolis, V.; Perra, A. Exploring the Binding Ability of Polyammonium Hosts for Anionic Substrates: Selective Size-Dependent Recognition of Different Phosphate Anions by Bis-macrocyclic Receptors. *Inorg. Chem.* **2011**, *50*, 7202–7216. [CrossRef]

39. Yoo, S.; Kim, S.; Eom, M.S.; Kang, S.; Lim, S.-H.; Han, M.S. Development of a highly sensitive colorimetric thymidine triphosphate chemosensor using gold nanoparticles and the p-xylyl-bis(Hg2+-cyclen) complex: Improved selectivity by metal ion tuning. *Tetrahedron Lett.* **2016**, *57*, 4484–4487. [CrossRef]

40. Zhao, X.J.; He, R.X.; Li, Y.F. A terbium(III)-organic framework for highly selective sensing of cytidine triphosphate. *Analyst* **2012**, *137*, 5190–5192. [CrossRef]

41. Gupta, A.K.; Dhir, A.; Pradeep, C.P. Ratiometric Detection of Adenosine-5′-triphosphate (ATP) and Cytidine-5′-triphosphate (CTP) with a Fluorescent Spider-Like Receptor in Water. *Eur. J. Org. Chem.* **2015**, *2015*, 122–129. [CrossRef]

42. Morozov, B.S.; Oshchepkov, A.S.; Klemt, I.; Agafontsev, A.M.; Krishna, S.; Hampel, F.; Xu, H.-G.; Mokhir, A.; Guldi, D.; Kataev, E. Supramolecular Recognition of Cytidine Phosphate in Nucleotides and RNA Sequences. *JACS Au* **2023**, *3*, 964–977. [CrossRef]

43. Kim, H.N.; Moon, J.H.; Kim, S.K.; Kwon, J.Y.; Jang, Y.J.; Lee, J.Y.; Yoon, J. Fluorescent sensing of triphosphate nucleotides via anthracene derivatives. *J. Org. Chem.* **2011**, *76*, 3805–3811. [CrossRef] [PubMed]

44. Roy, I.; David, A.H.G.; Das, P.J.; Pe, D.J.; Stoddart, J.F. Fluorescent cyclophanes and their applications. *Chem. Soc. Rev.* **2022**, *51*, 5557–5605. [CrossRef] [PubMed]

45. Tay, H.M.; Beer, P. Optical sensing of anions by macrocyclic and interlocked hosts. *Org. Biomol. Chem.* **2021**, *19*, 4652–4677. [CrossRef]

46. Wang, D.-X.; Wang, M.-X. Exploring Anion-π Interactions and Their Applications in Supramolecular Chemistry. *Acc. Chem. Res.* **2020**, *53*, 1364–1380. [CrossRef] [PubMed]

47. Xiong, S.; He, Q. Photoresponsive macrocycles for selective binding and release of sulfate. *Chem. Commun.* **2021**, *57*, 13514–13517. [CrossRef] [PubMed]

48. Lichosyt, D.; Dydio, P.; Jurczak, J. Azulene-Based Macrocyclic Receptors for Recognition and Sensing of Phosphate Anions. *Chem. Eur. J.* **2016**, *22*, 17673–17680. [CrossRef]

49. Katayev, E.A.; Myshkovskaya, E.N.; Boev, N.V.; Khrustalev, V.N. Anion binding by pyrrole–pyridine-based macrocyclic polyamides. *Supramol. Chem.* **2008**, *20*, 619–624. [CrossRef]

50. Flood, A.H. Creating molecular macrocycles for anion recognition. *Beilstein J. Org. Chem.* **2016**, *12*, 611–627. [CrossRef]

51. Evans, N.H.; Beer, P.D. Advances in Anion Supramolecular Chemistry: From Recognition to Chemical Applications. *Angew. Chem. Int. Ed.* **2014**, *53*, 11716–11754. [CrossRef]

52. Sarkar, S.; Ballester, P.; Spektor, M.; Kataev, E.A. Micromolar Affinity and Higher: Synthetic Host-Guest Complexes with High Stabilities. *Angew. Chem. Int. Ed.* **2022**, e202214705. [CrossRef]

53. Anda, C.; Angeles Martínez, M.; Llobet, A. A Systematic Evaluation of Molecular Recognition Phenomena: Part 5. Selective Binding of Tripolyphosphate and ATP to Isomeric Hexaazamacrocyclic Ligands Containing Xylylic Spacers. *Supramol. Chem.* **2005**, *17*, 257–266. [CrossRef]

54. Zhang, H.; Cheng, L.; Nian, H.; Du, J.; Chen, T.; Cao, L. Adaptive chirality of achiral tetraphenylethene-based tetracationic cyclophanes with dual responses of fluorescence and circular dichroism in water. *Chem. Commun.* **2021**, *57*, 3135–3138. [CrossRef] [PubMed]

55. Dhaenens, M.; Lehn, J.-M.; Vigneron, J.-P. Molecular Recognition of Nucleosides, Nucleotides and Anionic Planar Substrates by a Water-soluble Bis-intercaland-type Receptor Molecule. *J. Chem. Soc. Perkin Trans. 2* **1993**, *7*, 1379–1381. [CrossRef]

56. Neelakandan, P.P.; Nandajan, P.C.; Subymol, B.; Ramaiah, D. Study of cavity size and nature of bridging units on recognition of nucleotides by cyclophanes. *Org. Biomol. Chem.* **2011**, *9*, 1021–1029. [CrossRef] [PubMed]

57. van Eker, D.; Samanta, S.K.; Davis, A.P. Aqueous recognition of purine and pyrimidine bases by an anthracene-based macrocyclic receptor. *Chem. Commun.* **2020**, *56*, 9268–9271. [CrossRef] [PubMed]

58. Neelakandan, P.P.; Hariharan, M.; Ramaiah, D. A supramolecular ON-OFF-ON fluorescence assay for selective recognition of GTP. *J. Am. Chem. Soc.* **2006**, *128*, 11334–11335. [CrossRef]

59. Moreno-Corral, R.; Lara, K.O. Complexation Studies of Nucleotides by Tetrandrine Derivatives Bearing Anthraquinone and Acridine Groups. *Supramol. Chem.* **2008**, *20*, 427–435. [CrossRef]

60. Rhaman, M.M.; Powell, D.R.; Hossain, M.A. Supramolecular Assembly of Uridine Monophosphate (UMP) and Thymidine Monophosphate (TMP) with a Dinuclear Copper(II) Receptor. *ACS Omega* **2017**, *2*, 7803–7811. [CrossRef]

61. Ramaiah, D.; Neelakandan, P.P.; Nair, A.K.; Avirah, R.R. Functional cyclophanes: Promising hosts for optical biomolecular recognition. *Chem. Soc. Rev.* **2010**, *39*, 4158–4168. [CrossRef]

62. Agafontsev, A.M.; Shumilova, T.A.; Rüffer, T.; Lang, H.; Kataev, E.A. Anthracene-Based Cyclophanes with Selective Fluorescent Responses for TTP and GTP: Insights into Recognition and Sensing Mechanisms. *Chem. Eur. J.* **2019**, *25*, 3541–3549. [CrossRef]

63. Agafontsev, A.M.; Shumilova, T.A.; Oshchepkov, A.S.; Hampel, F.; Kataev, E.A. Ratiometric Detection of ATP by Fluorescent Cyclophanes with Bellows-Type Sensing Mechanism. *Chem. Eur. J.* **2020**, *26*, 9991–9997. [CrossRef] [PubMed]

64. Agafontsev, A.M.; Oshchepkov, A.S.; Shumilova, T.A.; Kataev, E.A. Binding and Sensing Properties of a Hybrid Naphthalimide-Pyrene Aza-Cyclophane towards Nucleotides in an Aqueous Solution. *Molecules* **2021**, *26*, 980. [CrossRef] [PubMed]

65. Kataev, E.A. Converting pH probes into "turn-on" fluorescent receptors for anions. *Chem. Commun.* **2023**, *59*, 1717–1727. [CrossRef] [PubMed]

66. Granzhan, A.; Kotera, N.; Teulade-Fichou, M.-P. Finding needles in a basestack: Recognition of mismatched base pairs in DNA by small molecules. *Chem. Soc. Rev.* **2014**, *43*, 3630–3665. [CrossRef] [PubMed]

67. Granzhan, A.; Largy, E.; Saettel, N.; Teulade-Fichou, M.-P. Macrocyclic DNA-mismatch-binding ligands: Structural determinants of selectivity. *Chem. Eur. J.* **2010**, *16*, 878–889. [CrossRef]

68. Kotera, N.; Granzhan, A.; Teulade-Fichou, M.-P. Comparative study of affinity and selectivity of ligands targeting abasic and mismatch sites in DNA using a fluorescence-melting assay. *Biochimie* **2016**, *128–129*, 133–137. [CrossRef]

69. Schlosser, J.; Ihmels, H. Ligands for Abasic-Site containing DNA and their Use as Fluorescent Probes. *Curr. Org. Synth.* **2023**, *20*, 96–113. [CrossRef]

70. Yaragorla, S.; Singh, G.; Dada, R. C(sp3)–H functionalization of methyl azaarenes: A calcium-catalyzed facile synthesis of (E)-2-styryl azaarenes and 2-aryl-1,3-bisazaarenes. *Tetrahedron Lett.* **2015**, *56*, 5924–5929. [CrossRef]

71. Seo, J.; Park, S.-R.; Kim, M.; Suh, M.C.; Lee, J. The role of electron-transporting Benzo[f]quinoline unit as an electron acceptor of new bipolar hosts for green PHOLEDs. *Dyes Pigm.* **2019**, *162*, 959–966. [CrossRef]

72. Brouwer, A.M. Standards for photoluminescence quantum yield measurements in solution (IUPAC Technical Report). *Pure Appl. Chem.* **2011**, *83*, 2213–2228. [CrossRef]

73. Buettelmann, B.; Alanine, A.; Bourson, A.; Gill, R.; Heitz, M.-P.; Mutel, V.; Pinard, E.; Trube, G.; Wyler, R. 2-Styryl-pyridines and 2-(3,4-Dihydro-naphthalen-2-yl)pyridines as Potent NR1/2B Subtype Selective NMDA Receptor Antagonists. *Chimia* **2004**, *58*, 630. [CrossRef]

74. Mittapalli, R.R.; Namashivaya, S.S.R.; Oshchepkov, A.S.; Kuczyńska, E.; Kataev, E.A. Design of anion-selective PET probes based on azacryptands: The effect of pH on binding and fluorescence properties. *Chem. Commun.* **2017**, *53*, 4822–4825. [CrossRef]

75. Beggiato, G.; Favaro, G.; Mazzucato, U. Acid-base equilibria of dipyridylethylenes studied by absorption and fluorescence spectrometry. *J. Heterocycl. Chem.* **1970**, *7*, 583–587. [CrossRef]

76. Zhang, C.; Li, M.; Liang, W.; Zhang, G.; Fan, L.; Yao, Q.; Shuang, S.; Dong, C. Substituent Effect on the Properties of pH Fluorescence Probes Containing Pyridine Group. *ChemistrySelect* **2019**, *4*, 5735–5739. [CrossRef]

77. Budyka, M.F.; Fedulova, J.A.; Gavrishova, T.N.; Li, V.M.; Potashova, N.I.; Tovstun, S.A. 2+2 Photocycloaddition in a bichromophoric dyad: Photochemical concerted forward reaction following Woodward-Hoffmann rules and photoinduced stepwise reverse reaction of the ring opening via predissociation. *Phys. Chem. Chem. Phys.* **2022**, *24*, 24137–24145. [CrossRef]

78. Chen, D.; Zhong, C.; Zhao, Y.; Nan, L.; Liu, Y.; Qin, J. A two-dimensional molecule with a large conjugation degree: Synthesis, two-photon absorption and charge transport ability. *J. Mater. Chem. C* **2017**, *5*, 5199–5206. [CrossRef]

79. Budyka, M.F.; Potasheva, N.I.; Gavrishova, T.N.; Li, V.M. Photoisomerization and [2 + 2] photocycloaddition in bichromophoric styrylbenzoquinoline dyads with o-xylylene bridge group. *High Energy Chem.* **2017**, *51*, 201–208. [CrossRef]

80. Budyka, M.F.; Gavrishova, T.N.; Li, V.M.; Potashova, N.I.; Fedulova, J.A. Emissive and reactive excimers in a covalently-linked supramolecular multi-chromophoric system with a balanced rigid-flexible structure. *Spectrochim. Acta Part A Mol. Biomol. Spectrosc.* **2022**, *267*, 120565. [CrossRef] [PubMed]

81. Tripathy, M.; Subuddhi, U.; Patel, S. A styrylpyridinium dye as chromogenic and fluorogenic dual mode chemosensor for selective detection of mercuric ion: Application in bacterial cell imaging and molecular logic gate. *Dyes Pigm.* **2020**, *174*, 108054. [CrossRef]

82. Sivakumar, R.; Lee, N.Y. Paper-Based Fluorescence Chemosensors for Metal Ion Detection in Biological and Environmental Samples. *BioChip J.* **2021**, *15*, 216–232. [CrossRef]

83. Bazany-Rodríguez, I.J.; Salomón-Flores, M.K.; Bautista-Renedo, J.M.; González-Rivas, N.; Dorazco-González, A. Chemosensing of Guanosine Triphosphate Based on a Fluorescent Dinuclear Zn(II)-Dipicolylamine Complex in Water. *Inorg. Chem.* **2020**, *59*, 7739–7751. [CrossRef] [PubMed]

84. Viviano-Posadas, A.O.; Romero-Mendoza, U.; Bazany-Rodríguez, I.J.; Velázquez-Castillo, R.V.; Martínez-Otero, D.; Bautista-Renedo, J.M.; González-Rivas, N.; Galindo-Murillo, R.; Salomón-Flores, M.K.; Dorazco-González, A. Efficient fluorescent recognition of ATP/GTP by a water-soluble bisquinolinium pyridine-2,6-dicarboxamide compound. Crystal structures, spectroscopic studies and interaction mode with DNA. *RSC Adv.* **2022**, *12*, 27826–27838. [CrossRef] [PubMed]

85. Dorazco-González, A.; Alamo, M.F.; Godoy-Alcántar, C.; Höpfl, H.; Yatsimirsky, A.K. Fluorescent anion sensing by bisquinolinium pyridine-2,6-dicarboxamide receptors in water. *RSC Adv.* **2014**, *4*, 455–466. [CrossRef]

86. Steenken, S.; Jovanovic, S.V. How Easily Oxidizable Is DNA? One-Electron Reduction Potentials of Adenosine and Guanosine Radicals in Aqueous Solution. *J. Am. Chem. Soc.* **1997**, *119*, 617–618. [CrossRef]

87. Seidel, C.A.M.; Schulz, A.; Sauer, M.H.M. Nucleobase-Specific Quenching of Fluorescent Dyes. 1. Nucleobase One-Electron Redox Potentials and Their Correlation with Static and Dynamic Quenching Efficiencies. *J. Phys. Chem.* **1996**, *100*, 5541–5553. [CrossRef]

88. Hu, P.; Yang, S.; Feng, G. Discrimination of adenine nucleotides and pyrophosphate in water by a zinc complex of an anthracene-based cyclophane. *Org. Biomol. Chem.* **2014**, *12*, 3701–3706. [CrossRef] [PubMed]

89. Lohani, C.R.; Kim, J.-M.; Chung, S.-Y.; Yoon, J.; Lee, K.-H. Colorimetric and fluorescent sensing of pyrophosphate in 100% aqueous solution by a system comprised of rhodamine B compound and Al$_3^+$ complex. *Analyst* **2010**, *135*, 2079–2084. [CrossRef]

90. MacDougall, D.; Crummett, W.B. Guidelines for data acquisition and data quality evaluation in environmental chemistry. *Anal. Chem.* **1980**, *52*, 2242–2249. [CrossRef]